

DAYSIDE NEUTRAL WINDS IN THE QUIET *E*-REGION
DEDUCED FROM THE EISCAT RADAR DATA
(EXTENDED ABSTRACT)

Sawako MAEDA¹, Hitoshi FUJIWARA¹ and Satonori NOZAWA²

¹Kyoto University of Art and Design, Uryuyama, Kitashirakawa, Sakyo-ku, Kyoto 606-8271

²Solar-Terrestrial Environment Laboratory, Nagoya University, Honohara, Toyokawa 442-8507

Momentum balance of the *E*-region neutral gases is characterized basically by a balance between the pressure gradient force and the Coriolis force (including the centrifugal force), and the geostrophic balance is set up. At high latitudes, however, the effects of the ion drag complicate the balance of forces, particularly in the region lower than 120 km where the Hall drag dominates the Pedersen drag (LARSEN and WALTERSCHEID, 1995).

Rocket experiments for the high-latitude neutral wind measurements revealed the large horizontal wind shear in the vertical direction between 110 and 120 km height in response to the postmidnight diffuse aurora (LARSEN *et al.*, 1995). The jetlike wind feature between 115 and 120 km height was also observed. These features are not predicted by any tidal models nor by the simulation of the high-latitude forcing (BRINKMAN *et al.*, 1995). It is inferred that an enhancement of the ion drag due to the particle precipitation may modify the geostrophic balance (LARSEN and WALTERSCHEID, 1995). So far, the effects of ion drag on the neutral momentum balance in the high-latitude dayside *E*-region have not been investigated.

In order to examine the validity of the geostrophic balance at high-latitudes, it is important to analyze the dayside *E*-region neutral winds during a geomagnetic quiet period and compare the nightside winds. The EISCAT IS radar observations provide the neutral wind data with the vertical resolution of 3 km throughout a day. The present paper will discuss the dayside neutral winds on June 15/16, 1993 by using the database of EISCAT Common Program 2 (CP2). The period of June 15/16 was geomagnetically quiet; the *Ap* index was 5 on June 15 and 3 on June 16, respectively. The *AE* index was less than 200 nT. The DST index ranged from -7 nT to 5 nT, and the convective electric field was less than 8 mV m⁻¹.

To obtain the neutral velocity in the region between 98 and 119 km altitude, the ion velocity in the specified region was used along with the electric field deduced from the ion velocity at 278 km height. The neutral horizontal velocity was derived from the ion momentum balance equation neglecting the ambipolar diffusion;

$$V = v_p - \Omega_i (\mathbf{E} + v_p \times \mathbf{B}) / (|\mathbf{B}| \nu_{in}), \quad (1)$$

where $\Omega_i = e|\mathbf{B}|/m_i$. V is the neutral velocity, v_p is the ion velocity, \mathbf{B} is the magnetic field, \mathbf{E} is the electric field, m_i is the ion mass, e is the electric charge, ν_{in} is the ion-neutral collision frequency calculated according to SCHUNK and WALKER (1973). LILLENSTEN *et al.* (1992) showed that the nighttime ambipolar diffusion velocity is small below 240 km compared to the velocity parallel to the geomagnetic field.

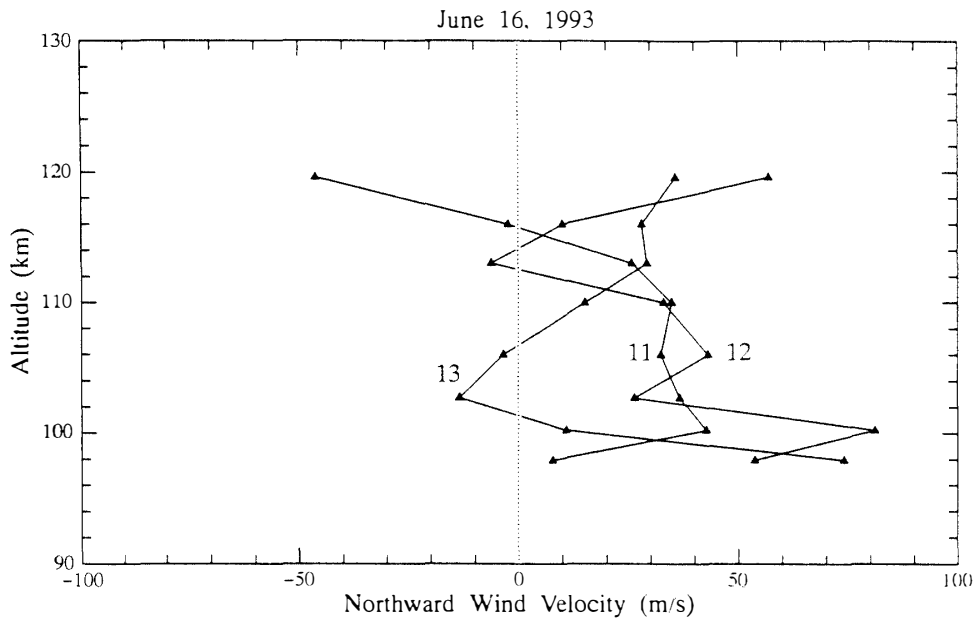


Fig. 1. Height profiles of the hourly averaged northward wind at 11, 12 and 13 UT.

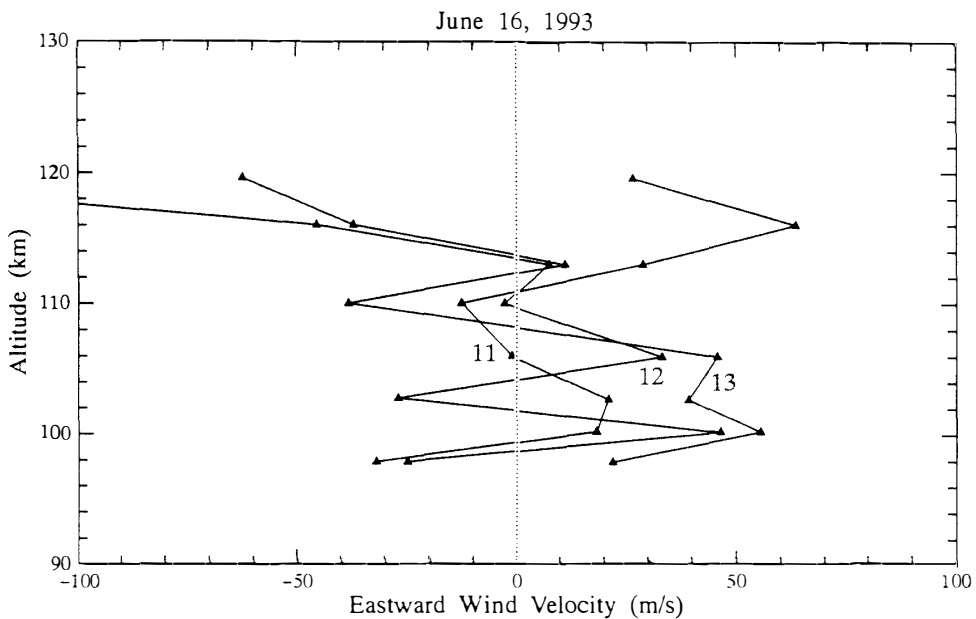


Fig. 2. Same as in Fig. 1, but for the eastward wind.

Figures 1 and 2 show the profiles of the hourly averaged meridional and zonal winds at three universal times from 11 to 13 UT, respectively. The meridional wind was generally northward, and its magnitude was about 40 ms^{-1} . The zonal wind was eastward below 110 km, but tended to be westward above 116 km height except for 11 UT. The magnitude of the eastward wind was about 40 ms^{-1} around 103 km, and the westward wind was up to 100 ms^{-1} at 119 km altitude. The daytime winds do not exhibit a strong shear compared to the nighttime winds as observed during the postmidnight diffuse aurora (LARSEN *et al.*, 1995). The height dependence of the horizontal velocities are reasonably consistent with the results of statistic analyses for

quiet summer days by BREKKE *et al.* (1994) and NOZAWA *et al.* (1997).

In order to discuss the validity of the geostrophic balance, the relationship between the pressure gradient force and the wind velocity must be examined. The pressure gradient force is derived from the momentum conservation equation of the neutral gases. The momentum equation in a steady state is given as follows;

$$-2\Omega \times V - \nabla P / \rho + (J \times B) / \rho - k_R V - \mu (\delta^2 V / \delta^2 z) / \rho = 0, \quad (2)$$

where Ω is the angular velocity of the Earth rotation, P is the pressure, J is the current density, ρ is the density, μ is the viscosity coefficient including molecular and eddy viscosity. The molecular viscosity coefficient is given by BANKS and KOCKARTS (1973). The eddy viscosity coefficient is related to the eddy diffusion coefficient and the Prandtl number. The eddy diffusion coefficient is taken from the formulae by SHIMAZAKI (1971), and the Prandtl number is chosen to be 2. The so-called 'wave drag' is expressed as Rayleigh friction, $-k_R V$. The coefficient k_R is assumed to be 10^{-6} s^{-1} , which is one order of magnitude smaller than the viscosity coefficient. FORBES *et al.* (1991) derived a Rayleigh friction parameterization of the gravity wave stress in the order of magnitude from 10^{-6} to 10^{-5} s^{-1} in the height range between 100 and 200 km. It is noted that the characteristic length of the vertical variations of the horizontal velocities is approximated by the scale height H . Hence, the second derivative of V , appeared in the fifth term on the left hand side of eq. (2), can be expressed as follows;

$$\delta^2 V / \delta^2 z = V / H^2. \quad (3)$$

The neutral velocities derived from the eq. (1) were substituted into the eq. (2) to calculate the pressure gradient force. The neutral temperature was assumed to be equal to the temperature of ion gases. The ion temperature was obtained from the EISCAT CP2 data base. The electric conductivities, the neutral gas density and composition were

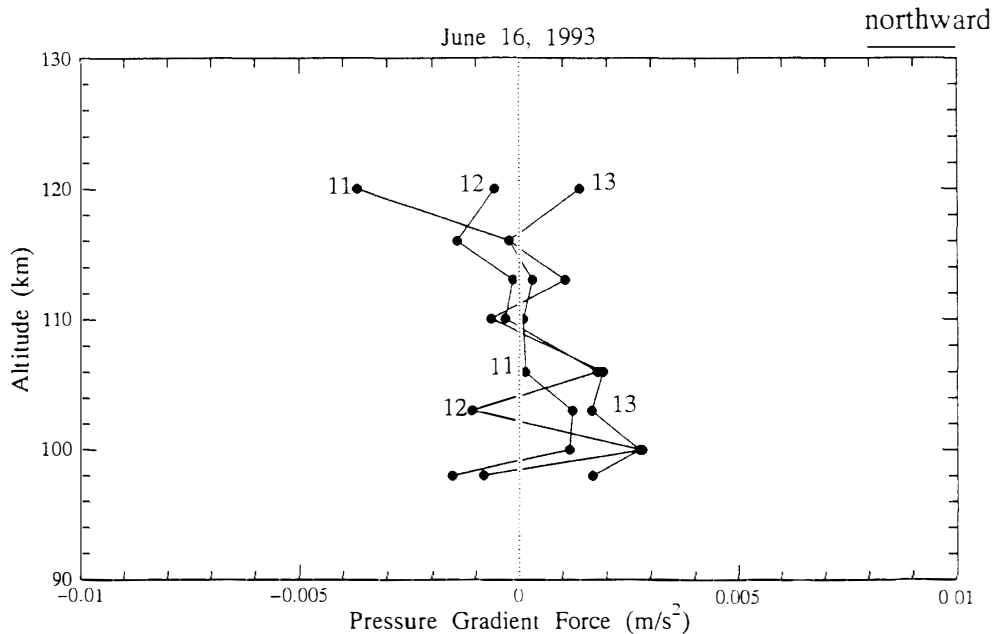


Fig. 3. Height profiles of the meridional pressure gradient force at 11, 12 and 13 UT. The positive is northward.

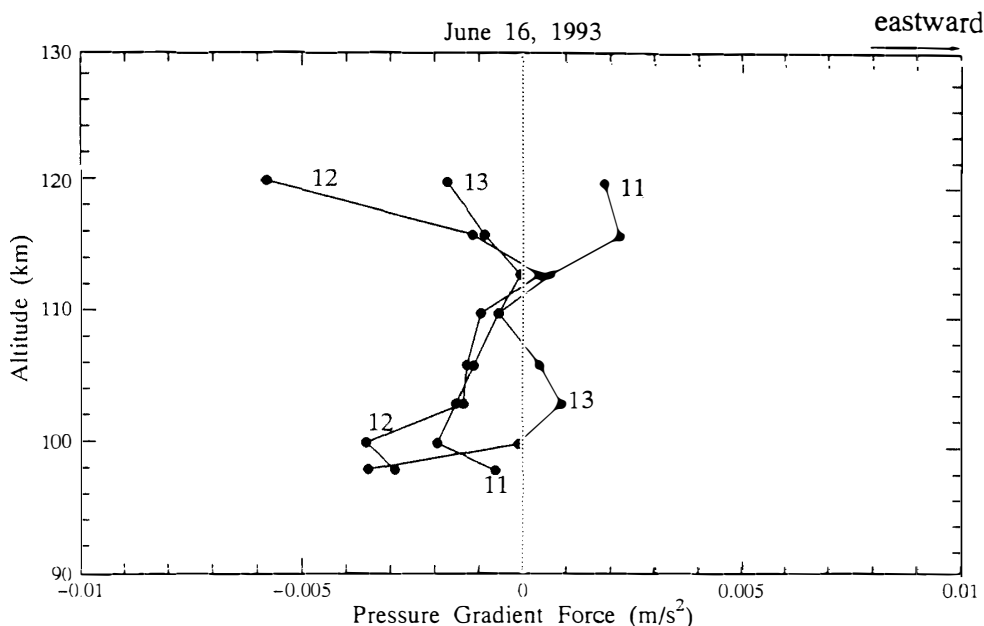


Fig. 4. Same as in Fig. 3, but for the zonal pressure gradient force. The positive is eastward.

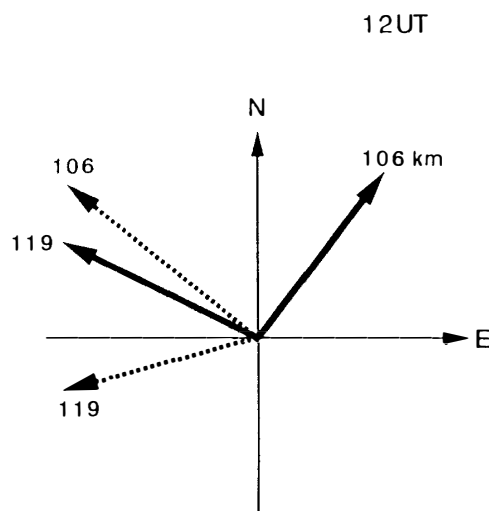


Fig. 5. Vector representation of wind (\rightarrow) and pressure gradient force ($\cdots\rightarrow$) at 106 and 119 km height. Magnitude of wind and strength of force are normalized.

computed from the MSIS 90 model. The meridional and zonal pressure gradient forces are shown in Figs. 3 and 4, respectively. Figure 5 represents the relationship between the pressure gradient force and wind velocity above and below 110 km height at 12 UT.

The pressure gradient force was in the northwest direction below 110 km height. The geostrophic winds under the northwest pressure gradient force are northeastward, consistent with the measured winds. Above 110 km, the pressure gradient force tended to be southwest-west and the geostrophic winds flow towards northwest-north. The measured winds was northwest-west. The observed deviation of the neutral wind vector from that of the geostrophic wind suggests that the ion drag and/or the viscous friction retards the winds, which now has a component across the isobars.

Figure 6 compares the magnitudes of the Coriolis parameter (f), the normalized electric conductivities, $D_p (= \sigma_p B^2 / \rho)$ and $D_h (= \sigma_h B^2 / \rho)$, and the kinematic viscosity

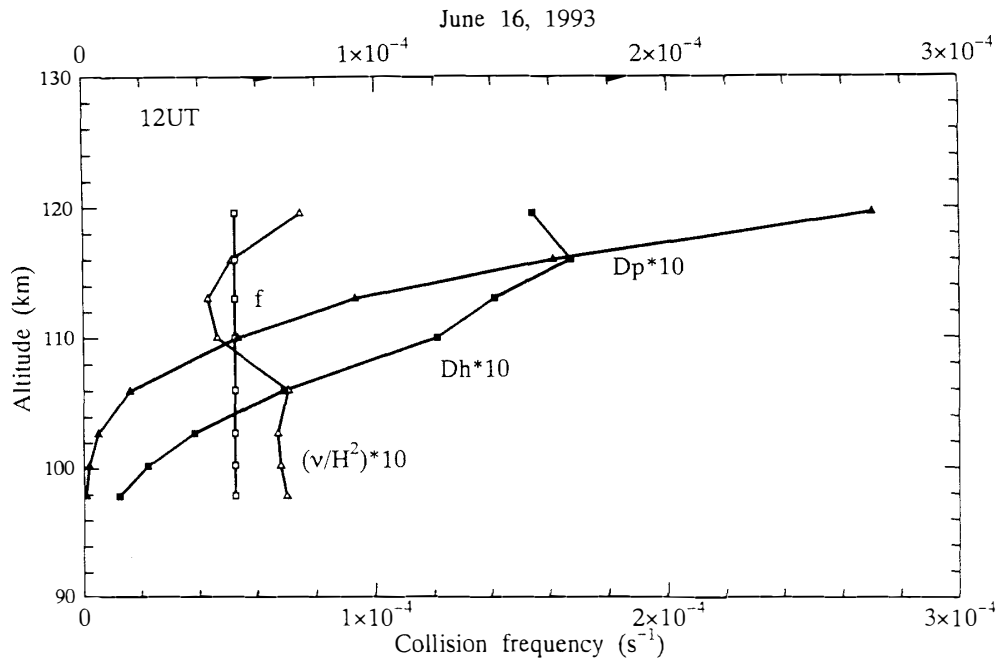


Fig. 6. Height profiles of the Coriolis parameter (f) and of the coefficients of the viscosity ($10 \times \nu/H^2$), Pedersen drag ($10 \times D_p$) and Hall drag ($10 \times D_h$) at 12 UT.

coefficient (ν/H^2), where σ_p and σ_h are the Pedersen and Hall conductivities, respectively. The quantities D_p and D_h are the coefficients of the Pedersen drag and Hall drag, respectively. The kinematic viscosity coefficient is one order of magnitude smaller than the Coriolis parameter throughout the region. If the characteristic length of the vertical wind shear is one third of the scale height, the viscous force becomes the same order of magnitude as the Coriolis force. The magnitude of the coefficient of Hall drag D_h is about 30% of the Coriolis parameter f above 115 km, which implies that the coefficient of Hall drag effectively reduces the Coriolis parameter even at daytime as shown by LARSEN and WALTERSCHEID (1995) for the case with postmidnight diffuse aurora. It is found that the coefficient of daytime Pedersen drag becomes the same order of magnitude above 115 km height. The Pedersen drag largely affects the momentum balance and deviates the neutral winds from the geostrophic winds.

It is summarized here that the neutral horizontal velocity is represented by the geostrophic winds below 110 km, but above this level the ion drag affects the geostrophic balance even in the geomagnetically quiet times due to the daytime increase in electric conductivities, and the neutral horizontal winds begin to flow partly across the isobars. The pressure gradient forces shown in Figs. 3 and 4 correspond to the horizontal temperature gradients of the order of 0.01 K km^{-1} . It is desirable to investigate whether the horizontal temperature gradient is consistent with the above estimation.

Acknowledgments

We are indebted to the Director and staff of EISCAT for operating the facility and supplying the data. We also thank R. FUJII for providing us with the EISCAT data and his valuable comments.

References

- BANKS, P. M. and KOCKARTS, G. (1973): *Aeronomy*. Part B. New York, Academic.
- BREKKE, A., NOZAWA, S. and SPARR, T. (1994): Studies of the *E* region neutral wind in the quiet auroral ionosphere. *J. Geophys. Res.*, **99**, 8801–8825.
- BRINKMAN, D. G., WALTERSCHEID, R. L., LYONS, L. R., KAYSER, D. C., CHRISTENSEN, A. B., SHARBER, J. R., FRAHM, R. A. and LARSEN, M. F. (1995): *E* region neutral winds in the postmidnight diffuse aurora during the Atmospheric Response in Aurora 1 rocket campaign. *J. Geophys. Res.*, **100**, 17309–17320.
- FORBES, J. M., GU, J. and MIYAHARA, S. (1991): On the interactions between gravity waves and the diurnal propagating tide. *Planet. Space Sci.*, **39**, 1249–1257.
- LARSEN, M. F. and WALTERSCHEID, R. L. (1995): Modified geostrophy in the thermosphere. *J. Geophys. Res.*, **100**, 17321–17329.
- LARSEN, M. F., MARSHALL, T. R., MIKKELSEN, I. S., EMERY, B. A., CHRISTENSEN, A., KAYSER, D., HECHT, J., LYONS, L. and WALTERSCHEID, R. (1995): Atmospheric Response in Aurora Experiment: Observations of *E* and *F* region neutral winds in a region of postmidnight diffuse aurora. *J. Geophys. Res.*, **100**, 17299–17308.
- LILENSTEN J., THUILLIER, G., LATHUILLERE, C., KOFMAN, W., FAULIOT, V. and HERSE, M. (1992): EISCAT-MICADO coordinated measurements of meridional wind. *Ann. Geophys.*, **10**, 603–618.
- NOZAWA, S., BREKKE, A. and FUJII, R. (1997): Studies of the *E* region neutral wind in the auroral ionosphere using two long-run data. *J. Geomagn. Geoelectr.*, **49**, 641–673.
- SHIMAZAKI, T. (1971): Effective eddy diffusion coefficient and atmospheric composition in the lower thermosphere. *J. Atmos. Terr. Phys.*, **33**, 1383–1401.
- SCHUNK, R. W. and WALKER, J.C.G. (1973): Theoretical ion densities in the lower ionosphere. *Planet. Space Sci.*, **21**, 1875–1896.

(Received November 25, 1997; Revised manuscript accepted February 6, 1998)